

Effects of vertex corrections on diagrammatic approximations applied to the study of transport through a quantum dot

Leandro Tosi,¹ Pablo Roura-Bas,^{2,*} Ana María Llois,² and Luis O. Manuel³

¹*Centro Atómico Bariloche, Comisión Nacional de Energía Atómica, 8400 San Carlos de Bariloche, Argentina*

²*Centro Atómico Constituyentes, Comisión Nacional de Energía Atómica, 1650 San Martín, Argentina*

³*Instituto de Física Rosario, Universidad Nacional de Rosario, 2000 Rosario, Argentina*

(Received 26 July 2010; revised manuscript received 16 November 2010; published 2 February 2011)

In the present work, we calculate the conductance through a single quantum dot weakly coupled to metallic contacts. We use the spin-1/2 Anderson model to describe the quantum dot, while considering a finite Coulomb repulsion. We solve the interacting system using the noncrossing approximation (NCA) and the one-crossing approximation (OCA). We obtain the linear response conductance as a function of temperature and energy position of the localized level. From the comparison of both approximations we extract the role of the vertex corrections, which are introduced in the OCA calculations and neglected in the NCA scheme. As a function of the energy position, we observe that the diagrams omitted within the NCA are really important for appropriately describing transport phenomena in Kondo systems as well as in the mixed valence regime. On the other hand, as a function of temperature, the corrections introduced by the OCA partly recover the universal scaling properties known from numerical approaches such as the numerical renormalization group.

DOI: [10.1103/PhysRevB.83.073301](https://doi.org/10.1103/PhysRevB.83.073301)

PACS number(s): 73.63.Kv, 72.15.Qm, 75.20.Hr, 73.23.Hk

I. INTRODUCTION

Large- N expansions, with N representing the angular momentum degeneracy, are commonly used to solve the Anderson impurity model (AIM) and to study Kondo physics. In particular, the so-called noncrossing approximation (NCA) in its infinite Coulomb repulsion limit captures the formation of the Kondo resonance at finite temperatures.¹ When compared with the numerical renormalization group (NRG), the NCA scheme also provides the correct Kondo temperature (T_K).² This successful match results from the fact that the NCA collects, in a self-consistent way, all diagrams up to order $1/N$. However, it is well known that the Fermi liquid properties are not properly described.³⁻⁵

When a finite value of Coulomb repulsion U is allowed, the NCA gives a severely underestimated value of T_K .⁶ The leading crossing diagrams that restore the proper energy scale were introduced in the early work by Pruschke and Grewe within the framework of the enhanced-NCA (ENCA), also called the one-crossing approximation (OCA).⁷ Unlike NRG and quantum Monte Carlo, the OCA method can be extended to multiorbital systems without much numerical effort. It also works on the real axis and can go to temperatures far below the Kondo one. These features make the OCA a powerful impurity solver when combined with electronic structure calculations within the context of the dynamical mean-field theory.⁸

Due to the interesting advantages mentioned above, it is important to check the role of vertex corrections on diagrammatic techniques in the calculation of different properties. Recently, the influence of vertex functions incorporated by the OCA has already been studied for general lattice problems,⁹ multiorbital Anderson models¹⁰ and dynamic susceptibilities of the AIM,¹¹ among others.

In this work, we study the effect of vertex corrections on transport properties, in particular transport through a quantum dot (QD) weakly coupled to metallic contacts. The NCA results for the conductance, in the linear-response regime, were previously analyzed by Gerace *et al.*¹² The aim of our

contribution is to compare the equilibrium conductance, as a function of temperature and gate voltage, as calculated by NCA and OCA methods. Furthermore, we analyze the scaling properties of the conductance by comparison with the empirical formula extracted from NRG calculations.

We observe that the diagrams omitted within the NCA are really important for appropriately describing transport phenomena. Furthermore, the vertex corrections introduced by the OCA partially recover the universal scaling behavior of the conductance as a function of temperature.

The paper is organized as follows. In Sec. II we introduce the model and the calculation methods. In Sec. III we present and discuss numerical calculations. Finally, in Sec. IV some conclusions are drawn.

II. MODEL AND METHOD

To describe the system in which the QD is coupled to two leads we use the spin-1/2 Anderson Hamiltonian

$$H = \sum_{k\nu\sigma} \epsilon_{k\nu\sigma} c_{k\nu\sigma}^\dagger c_{k\nu\sigma} + \sum_{\sigma} E_d n_{d\sigma} + U n_{d\uparrow} n_{d\downarrow} + \sum_{k\nu\sigma} V_{k\nu} d_{\sigma}^\dagger c_{k\nu\sigma} + \text{H.c.}, \quad (1)$$

where the operator $c_{k\nu\sigma}^\dagger$ represents a conduction electron with momentum k and spin σ in lead ν ; $\nu = L, R$ labels the left and right leads; the operator d_{σ}^\dagger stands for an electron in the dot; and $n_{d\sigma}$ is the number operator for a given spin in the QD. The parameters E_d and U represent the energy of a single electron and the Coulomb repulsion in the dot, respectively. The coupling parameter and hybridization functions between the leads and the QD are given by $V_{k\nu}$ and $\Delta_{\nu}(\omega) \equiv \pi \sum_{k\sigma} V_{k\nu}^2 \delta(\omega - \epsilon_{k\nu\sigma})$, respectively.

Our starting point is an auxiliary particle representation of the Hamiltonian given by Eq. (1).¹³ In this representation, the physical operator is given by the following combination of the auxiliary particles: $d_{\sigma}^\dagger = f_{\sigma}^\dagger b + \sigma a^\dagger f_{-\sigma}$. Operators b ,

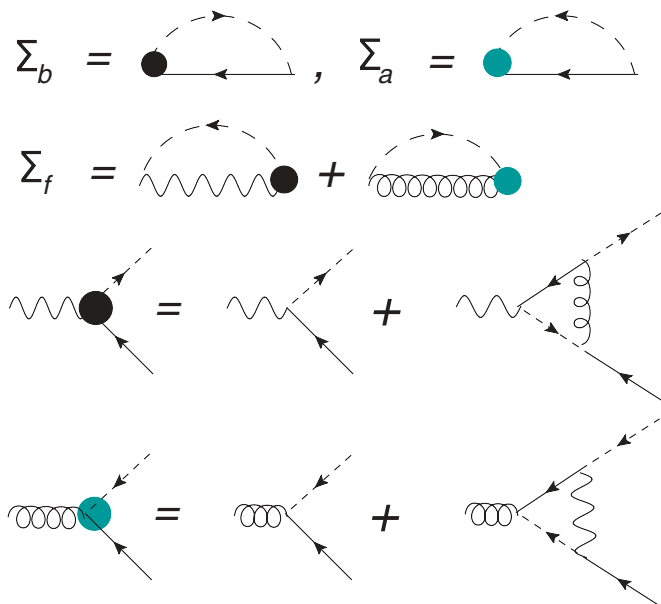


FIG. 1. (Color online) Sketch of the self-consistency OCA scheme for self-energies and vertex corrections of the auxiliary particles. The solid, wiggly, dashed, and curly lines stand for pseudofermion, empty boson, conduction electron, and doubly occupied boson propagators, respectively.

f_σ , and a label vacuum, single-, and doubly occupied states, respectively. Within the OCA scheme, the self-energies of the auxiliary particles and the vertex functions are obtained self-consistently. The set of OCA equations are sketched in Fig. 1.⁷

Once the spectral functions of the auxiliary particles are obtained, the physical spectral function, $\rho_d(\omega) = -1/\pi \mathcal{I}G_d(\omega)$, follows from direct convolution of the auxiliary ones and the vertex functions, where $G_d(\omega)$ represents the retarded Green function of the QD.

It should be pointed out that the NCA equations are recovered from the OCA when the vertex corrections are neglected in the self-energies and physical Green function bubbles.

As already stated, our aim in this work is to analyze the role of the crossing diagrams on equilibrium transport properties. In particular, the conductance through a QD within the linear-response regime is given by¹⁴

$$G = 4 \frac{e^2}{h} \pi \sum_{\sigma} \int_{-\infty}^{\infty} d\omega [-f'(\omega)] \Delta_T(\omega) \rho_d(\omega). \quad (2)$$

In Eq. (2), $\Delta_T(\omega) = \Delta_L(\omega)\Delta_R(\omega)/\Delta(\omega)$, where $\Delta(\omega) = \Delta_L(\omega) + \Delta_R(\omega)$ represents the total coupling between leads and the QD and $f(\omega) = 1/(1 + e^{\beta\omega})$ is the Fermi function.

III. NUMERICAL RESULTS

In this section, we present the results obtained for spectral density and conductance as a function of temperature and position of the QD level within both the NCA and OCA schemes. When solving the self-consistency equations, we consider the case of symmetric couplings, $\Delta_L = \Delta_R$, and the hybridization functions to be step functions $\Delta_\nu(\omega) =$

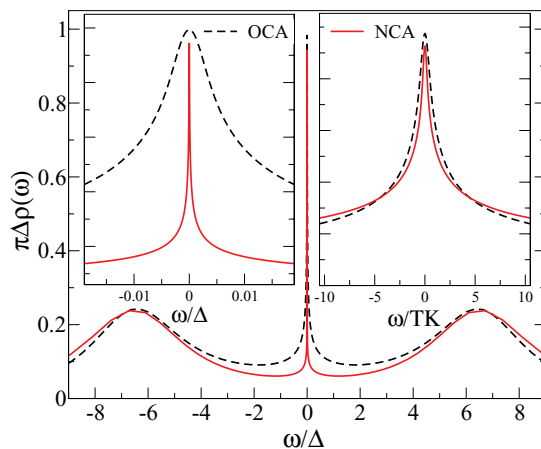


FIG. 2. (Color online) Physical spectral function of the QD for the symmetric case, $E_d = -U/2 = -6$ and $D = 20\Delta$. The insets show a zoom of the region near the Fermi energy $\omega = 0$.

$\Delta_\nu \theta(D - |\omega|)$ with bandwidth D several times larger than Δ_ν . From now on, we choose the total hybridization $\Delta = 1$ as our unit of energy.

The numerical procedure used to solve the NCA and OCA equations follows the method proposed by Kroha *et al.* to describe the spectral densities of the auxiliary and physical particles.¹⁵ The procedure guarantees the resolution of the sets of integral equations for the auxiliary particles' self-energies to a high degree of accuracy down to low temperatures.

As a first step, we obtain the physical spectral function for the symmetric Anderson model ($E_d = -U/2$) within the NCA and the OCA. Figure 2 shows the results for $E_d = -6$ at the same temperature $T = 0.1T_K$ in units of each T_K , with $T_K^{NCA} = 0.00017$ and $T_K^{OCA} = 0.009$. For the definition of Kondo temperature, T_K , we adopt the temperature for which $G(T_K) \equiv G_0/2$ with $G_0 = 2\frac{e^2}{h}$.

As it was shown previously by Haule *et al.*,⁶ from Fig. 2 it is clear that the charge-transfer peaks, located around E_d and $E_d + U$, are insensitive to vertex corrections. On the other hand, the width of the Kondo resonance peak (left inset of Fig. 2), which also represents the Kondo temperature, increases orders of magnitude within the OCA as compared to the NCA. The larger value of T_K provided by the OCA can be traced back to the incorporation of the lowest-order vertex corrections necessary to produce the correct Schrieffer-Wolff exchange coupling.

We are interested here in the modification induced on the conductance by the enhancement of the Kondo scale and on the different shape of the Kondo resonance when scaled by the corresponding T_K . In Fig. 3 we present the conductance as a function of the energy level E_d , which is proportional to gate voltage, in both NCA and OCA schemes at a high temperature, $T = 0.8$. Figure 3 also shows the NCA occupation of the QD as a function of E_d . We observe that there is no difference between NCA and OCA occupations. This results from the fact that this magnitude is a static one, that is, energy-integrated, and therefore weakly dependent on temperature. The value of the occupation number indicates the different regimes of the QD. In particular, $\langle n \rangle \sim 1$ stands for the Kondo regime. As it is seen, at this temperature value, there is no formation

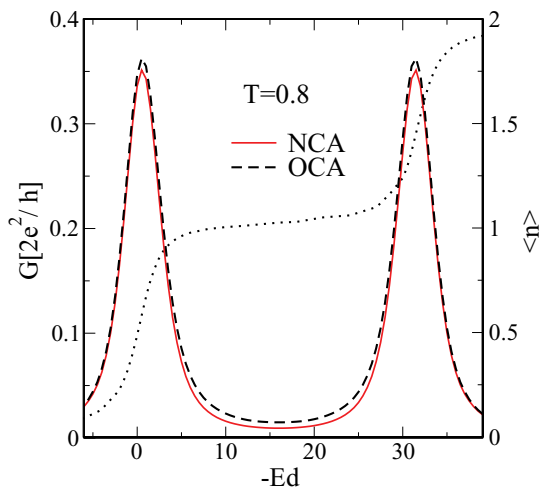


FIG. 3. (Color online) Conductance in the linear-response regime and occupation (dotted curve) of QD at high temperature, $T = 0.8\Delta$, as a function of the energy position E_d . Parameters: $U = 32, D = 43$.

of the Kondo resonance within NCA or within OCA. The conductance presents two separate peaks at the gate voltages for which the charge-transfer peaks traverse the Fermi level. Due to the absence of the Kondo peak at this temperature (see Fig. 1 of Ref. 12) there is no qualitative difference between NCA and OCA conductances, further reinforcing what we pointed in the spectral density of Fig. 2.

When the temperature decreases, due to the formation of the Kondo resonance at the Fermi level, the conductance valley showed in Fig. 3 tends to raise as soon as the occupation in the QD is close to one (this means within the Kondo regime). For low enough temperatures as compared to the Kondo one, the Kondo effect is fully developed and the Kondo peak of the spectral density reaches the limit imposed by Friedel's sum rule [$\rho(0) = 1/\pi\Delta$]. As a consequence, the conductance valley evolves into a plateau at G_0 . This feature of the conductance is found by solving the spectral density of the QD using, for example, the slave bosons approach and the NRG.¹⁶ In the present case, the effect of low but finite temperature is shown in Fig. 4 for $T = 0.013$ within the OCA. The conductance has a minimum at the symmetric case and then increases far from this due to the increment in the Kondo temperature. For the same absolute temperature, the NCA results still show a pronounced valley; left panel of Fig. 4. To obtain a similar behavior using the same set of parameters, it would be necessary to go to temperatures several orders of magnitude smaller than within the OCA.

When compared at the same temperature in units of each T_K for the symmetric case, right panel of Fig. 4, we observe a lower value of the NCA conductance at the symmetric point. This is related to the lower value of the spectral function at $\omega = 0$ as it is shown in Fig. 2. In this case, we present the calculations at $T = 0.2T_K$ of the symmetric case, for which the unitary limit is not exceeded by the OCA within the whole range of selected E_d values. Near the symmetric case, the NCA results increase faster than the OCA ones and when some charge fluctuations are allowed, we obtain a violation of the unitary limit for the NCA conductance. This represents an important improvement in the OCA performance over the NCA one.

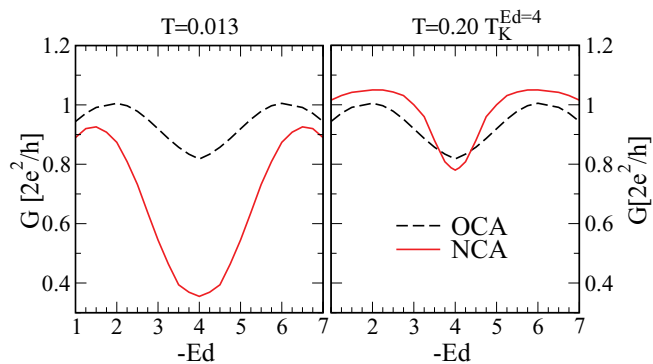


FIG. 4. (Color online) Conductance through the QD at low temperatures as a function of the energy position E_d . Parameters: $U = 8, D = 20$

As we mentioned previously, when comparing the spectral function in units of T_K (right inset of Fig. 2) and the conductance as a function of E_d for the same temperature in units of T_K (right panel of Fig. 4), the NCA and the OCA exhibit different scaling features. Thereafter, in what follows, we focus on the study of the universal scaling properties of the conductance as a function of temperature. NCA results for the universal behavior of the conductance as a function of T/T_K were previously analyzed for different values of the energy level E_d .¹² Also, for different values of Coulomb repulsion U close to the limit $U \rightarrow \infty$.¹⁷ In Fig. 5 we present the results for the conductance as a function of T/T_K for the symmetric case within the Kondo regime. In addition, we include the empirical formula for $G(T)$ extracted from NRG calculations for a spin-1/2,

$$G_E(T) = \frac{G(0)}{[1 + (2^{1/s} - 1)(T/T_K)^2]^s}, \quad (3)$$

with $s = 0.22$.¹⁸

Due to the overestimation of Friedel's sum rule within both diagrammatic schemes below a pathology scale $T_{\text{path}} \sim 0.1 - 0.01T_K$,¹¹ we restrict our scaling analysis up to $T = 0.1T_K$, where there is no violation of the unitary limit $G/G_0 = 1$. Below this temperature, we observe that the conductance still increases when saturation is expected; therefore it can

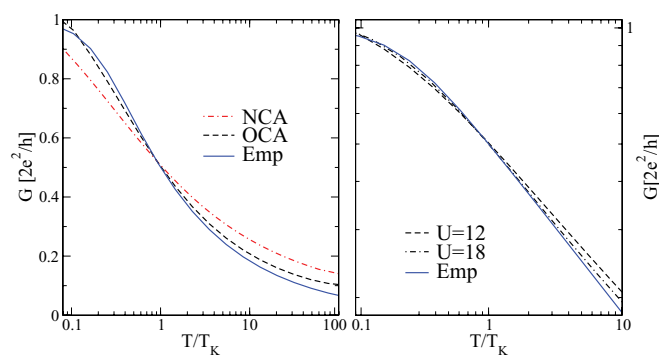


FIG. 5. (Color online) Conductance as a function of T/T_K for the symmetric Anderson model. Left panel: $E_d = 6, U = 12, D = 20$. The solid, dashed, and dot-dashed lines stand for NRG, OCA, and NCA techniques respectively. Right panel: OCA conductance for the symmetric case, $U = 12$, and far from this, $U = 18$ (dot-dashed line).

be considered as the limit of accuracy for calculating the conductance. As is shown in Fig. 5, left panel, we find that the NCA and OCA conductances follow different scaling behaviors in the whole range of temperatures. The OCA conductance is closer to the exact prediction of the NRG than the NCA is for both low and high temperatures. It must be noted that vertex corrections not only change the Kondo scale but also the whole temperature dependence. However, it can be observed from Fig. 5 that the vertex functions introduced by the OCA are not sufficient to recover the NRG prediction. At this point, a set of self-consistent vertex equations should be considered.⁶ As a last remark, it must be pointed out that while the NCA in its $U \rightarrow \infty$ limit follows the empirical law given by Eq. (3), Ref. 17, the finite U versions presented here fail for the symmetric case. The right panel of Fig. 5 shows the conductance for the symmetric case and for a larger value of U . We notice that for large U , the extra diagrams not included within the OCA give a small contribution and as a consequence the conductance agrees very well with the NRG prediction.

IV. CONCLUSIONS

In this work we obtain the conductance as a function of both temperature and gate voltage, for a quantum dot modeled by the Anderson impurity Hamiltonian. We calculate the spectral density of the quantum dot by using the finite Coulomb

repulsion noncrossing and one-crossing approximations. The comparison of both schemes lets us conclude about the role of vertex corrections when calculating transport properties. At high absolute temperatures there is no qualitative difference between NCA and OCA conductances as a function of gate voltage as well as between the occupations of the dot. On the contrary, at the same low temperature in units of each T_K , the results severely differ as a function of both, gate voltage, and temperature. This is related not only to the underestimated Kondo scale within the NCA, but also to the different height of the Kondo resonance and the rapid violation of Friedel's sum rule far from the symmetric case. Finally, when compared with the NRG results, the OCA conductance as a function of temperature is more reliable than the NCA one. For large values of the Coulomb repulsion, away from the symmetric case, the OCA and NRG conductances agree very well. However, close to the symmetric case, in order to recover the NRG prediction, it is still necessary to go beyond OCA corrections.

ACKNOWLEDGMENTS

Two of us (A.M.L. and L.O.M.) are supported by CONICET. This work was done within the framework of projects PIP 5254 and PIP 6016 of CONICET, and PICT 2006/483 and 33304 of the ANPCyT and UBACyT X123.

*roura@tandar.cnea.gov.ar

¹N. E. Bickers, *Rev. Mod. Phys.* **59**, 845 (1987).

²T. A. Costi, J. Kroha, and P. Wölfle, *Phys. Rev. B* **53**, 1850 (1996).

³F. B. Anders, *J. Phys. Condens. Matter* **7**, 2801 (1995).

⁴J. Kroha, P. Wölfle, and T. A. Costi, *Phys. Rev. Lett.* **79**, 261 (1997).

⁵S. Kirchner, J. Kroha, and P. Wölfle, *Phys. Rev. B* **70**, 165102 (2004).

⁶K. Haule, S. Kirchner, J. Kroha, and P. Wölfle, *Phys. Rev. B* **64**, 155111 (2001).

⁷Th. Pruschke and N. Grewe, *Z. Phys. B* **74**, 439 (1989).

⁸K. Haule, C. H. Yee, and K. Kim, *Phys. Rev. B* **81**, 195107 (2010).

⁹N. Grewe, S. Schmitt, T. Jabben, and F. B. Anders, *J. Phys. Condens. Matter* **20**, 365217 (2008).

¹⁰N. Grewe, T. Jabben, and S. Schmitt, *Eur. Phys. J. B* **68**, 23 (2009).

¹¹S. Schmitt, T. Jabben, and N. Grewe, *Phys. Rev. B* **80**, 235130 (2009).

¹²D. Gerace, E. Pavarini, and L. C. Andreani, *Phys. Rev. B* **65**, 155331 (2002).

¹³P. Coleman, *Phys. Rev. B* **29**, 3035 (1984).

¹⁴N. S. Wingreen and Y. Meir, *Phys. Rev. B* **49**, 11040 (1994).

¹⁵M. H. Hettler, J. Kroha, and S. Hershfield, *Phys. Rev. B* **58**, 5649 (1998).

¹⁶A. M. Lobos and A. A. Aligia, *Phys. Rev. B* **74**, 165417 (2006).

¹⁷P. Roura-Bas, *Phys. Rev. B* **81**, 155327 (2010).

¹⁸T. A. Costi, *Phys. Rev. Lett.* **85**, 1504 (2000).